Desalination and Water Treatment
www.deswater.com
doi: 10.1080/19443994.2013.853625

53 (2015) 430–445
January

Taylor & Francis
Taylor & Francis Group

Doehlert design as optimization approach for the removal of Pb(II) from aqueous solution by *Catalpa Speciosa* tree leaves: adsorption characterization

Javad Zolgharnein[a,*], Tahere Shariatmanesh[a], Neda Asanjarani[a], Abdolali Zolanvari[b]

[a]*Faculty of Science, Department of Chemistry, Arak University, Arak 38156-8-8394, Iran*
Tel. +98 86 3417701-2042; Fax: +98 86 34173406; email: j-zolgharnein@araku.ac.ir
[b]*Faculty of Science, Department of Physics, Arak University, Arak 38156-8-8394, Iran*

Received 17 April 2013; Accepted 3 October 2013

ABSTRACT

Catalpa speciosa tree leaves were used to remove Pb(II) from aqueous solutions. Removal process was optimized by applying experimental design strategy. Optimization was based on the application of a two-level full-factorial design for screening the significant variables followed by a Doehlert design to find out an appropriate model which leads to determine the optimum conditions. The empirical models were developed in terms of effective factors: pH, initial concentration of metal ion C_m and sorbent mass(s) have been found statistically adequate to describe the process responses, that is, removal percent and the capacity uptake of Pb(II). The multiresponse optimization of Pb(II) removal process has been carried out using desirability function approach. To this end, Derringer's desirability function (D) has been applied for mathematical optimization of the simultaneous multiresponse problem. Thus, the optimum conditions of Pb(II) removal process have been found as: pH = 4.43, s = 0.07 g, and C_m = 104 mg L^{-1}. Responses were confirmed by experiments 86 and 14.7 mg g^{-1} for $R\%$ and q, respectively. The morphology and structure of biosorbent during adsorption process was characterized by FT-IR spectroscopy, X-ray diffraction and scanning electron microscopy techniques. Experimental data were also fitted to various isotherm models. Potentiometric titration, pH_{PZC}, and the competitive effect of alkaline and alkaline earth metal ions during the loading of Pb(II) indicate that ion exchange is the predominant mechanism for the adsorption of Pb(II) by *C. speciosa* tree leaves.

Keywords: *Catalpa speciosa;* Desirability function; Doehlert design; Pb(II); Potentiometric titration

1. Introduction

Contamination of natural resources and wastewaters with industrial development by different pollutants has become a major concern today due to deleterious effects of contaminants on the environment and human health [1]. Lead is a toxic metal that has transformed in environment during different anthropogenic activities, such as mining, metal plating, photographic materials manufacturing, smelting, oil refinery, acid battery manufacturing, and explosive material manufacturing [2,3]. Emitted lead penetrates through drinking water, soil and even food. Since lead is nonbiodegradable, its accumulation in living tissues is highly probable, which may cause various diseases

*Corresponding author.

1944-3994/1944-3986 © 2013 Balaban Desalination Publications. All rights reserved.

and disorders [3]. The entrance of Pb(II) at high levels can cause convulsions, coma, and even death. Lead exposure's effect on fetuses and young children can be severe. It shows as delays in physical and mental development, lower IQ levels, shortening attention spans, and increased behavioral problems [4,5]. That is why in recent years, considerable attention has been devoted to reduce the Pb(II) concentration to low level required by water quality control standards. According to the current standard of Environmental Protection Agency, the maximum acceptable concentration of Pb(II) in drinking water is 0.05 mg L^{-1} [6]. Current methods for removing metals from aqueous solutions comprise chemical precipitation, chemical oxidation or reduction, ion exchange, filtration, electrochemical treatment, reverse osmosis, and membrane technologies [7]. These processes may become ineffective or extremely expensive, especially when the concentration of dissolved metals is in the range of 1–100 mg L^{-1} [7,8]. Biosorption as an alternative process offers several advantages such as low operation cost, minimum volume of chemical disposal and/or biological sludge to be disposed of, and high efficiency of detoxifying very dilute effluents [9]. Among the biosorbent categories, agricultural residue is more interesting due to some positive features like abundance, reusability, low cost, high efficiency, and simple operations [10–12]. Up to now, some biosorbents such as green algae *Spirogyra species* [6], *cotton waste* [13], *alga* [14], *seaweed* [15], *macrofungus* [16], *mansonia wood sawdust* [17], *palm kernel fiber* [18], and *tree leaves* [19] have been effectively utilized for the removal of Pb(II). Using tree leaves as a biosorbent, which is cheap and easily available in great supply, has been less attended by researchers [11,12,20]. There are only a few reports for the removal of Pb(II) by biosorbents, particularly by tree leaves such as *Catalpa speciosa*.

In this study, the potential of *C. speciosa* tree leaves in the removal of Pb(II) from aqueous solution as a new efficient sorbent was investigated. *C. speciosa* tree leave is an agricultural byproduct in a tremendous quantity in the north of Iran. Although, in previous reports, few tree leaves were considered as efficient sorbents for the removal of metal ions from polluted water, the exact interaction between the metal ions and sorbents has not been well addressed [20–22]. Thus, in order to investigate the mechanisms and recognize the functional groups involved in Pb(II) removal by *C. speciosa* tree leaves, potentiometric titration was used and released concomitant cations were determined. Moreover, in statistical viewpoint, the experimental design strategy offers a multivariate approach that shows many advantages over the conventional one-at-a-time method for the optimization of biosorption process. Among the experimental designs, Doehlert design offers some advantages over the other designs such as a lower number of runs and its ability to illustrate the role of effective factors and their interactions [23]. Therefore, the effect of major factors such as pH, initial concentration of Pb(II), temperature, and sorbent mass on the performance of *C. speciosa* tree leaves for the removal of Pb(II) are planned to be examined by Doehlert design. Furthermore, the desirability function approach is employed for simultaneous optimization of both responses (q, $R\%$).

Apart from the optimization of adsorption process, the other aims of this study are clarification of the mechanisms of binding Pb (II) to *C. speciosa* biomass upon finding its number of functional groups by potentiometric titration. Moreover, adsorbent sites and cell surface morphology were analyzed by means of FT-IR spectroscopy, scanning electron microscopy (SEM) and X-ray diffraction (XRD) analysis.

2. Materials and methods

2.1. Biosorbent materials

The *C. speciosa* tree leaves were collected from a coppice in suburb of Arak, an industrial city in the center of Iran. They were washed with tap water until the supernatant solution became clear then were rinsed using doubly distilled water and dried on a clean table at room temperature. The dried leaves were pulverized and sieved to 0.125–0.177 mm, then stored into a plastic bag.

2.2. Batch procedure

The stock solution of Pb(II) was prepared by dissolving appropriate quantities of $Pb(NO_3)_2$ salt in 5% (v/v) HNO_3. In a typical run, 10 mL of Pb(II) solution was used, and a known amount of dried biomass was added to each sample solution. The pH of solution was adjusted with HNO_3 or NaOH before the addition of biosorbent. Fresh dilutions were made for each study. The mixture was agitated at 300 rpm using a shaker at known temperature for 60 min and then filtered through 0.45-mm Whatman filter paper. In order to obtain the adsorption isotherms, batch experiments were conducted for Pb(II) aqueous solution with an initial concentration varying from 100 to 18,000 mg L^{-1} at pH = 5. The samples were mixed and retained for 60 min to attain the equilibrium. The resulting filtrate was analyzed for Pb(II) assay. The sorbent mass in these experiments was maintained constant at 18.9 g L^{-1}.

2.3. Metal analysis

The concentration of remained Pb(II) in solution after biosorption was determined by using atomic absorption spectrophotometer (Perkin–Elmer 2380, wavelength = 283.3 nm, slit = 0.7 nm). The capacity uptake q, amount of Pb(II) adsorbed onto unit weight of biosorbent, and removal percent %R were calculated using the following equations, respectively:

$$q = \frac{(C_0 - C)V}{s} \quad (1)$$

$$\%R = \frac{(C_0 - C) \times 100}{C_0} \quad (2)$$

where C_0 is the initial Pb(II) concentration (mg L^{-1}), C denotes the concentration of Pb(II) at any time t, V and s are volume of solution (L) and the sorbent mass (g), respectively.

2.4. Characterization of biosorbent

The chemical characterization of *C. speciosa* tree leaves was investigated by pH at point zero charge, potentiometric titration, FT-IR, XRD, SEM, and elemental analysis. The pH at point zero charge (pH_{PZC}) for the *C. speciosa* tree leaves was determined by boiling 100 mL deionized water for 20 min to eliminate dissolved CO_2 and quickly cooling and capping the solution. A sample of 0.2 g of tree leaves was placed in 15 mL of the CO_2-free water, then sealed and continuously agitated for 48 h at room temperature. Then the pH of the solution was measured, and this value was taken as the point of zero charge [24,25]. Potentiometric titration was performed using suspended leaves in deionized water (0.5 g in 90 mL), which preliminary was fluxed by N_2 under magnetic stirring for 15 min. A standardized HCl solution (0.1 mol L^{-1}) is added to each *C. speciosa* tree leave suspension to lower the initial pH from 5 to 2, and then titrated with a standard solution of NaOH 0.1 mol L^{-1}. The pH of the suspension was recorded after each addition of titrant (0.1 mL) by a pH-meter (Metrohm 721) till the equilibrium had been attained.

The Fourier transform infrared (FT-IR) spectra of biomass before and after loading Pb(II) was taken in the range of 400–4,000 cm^{-1} by using a Unicam-Galaxy series FT-IR 5,000, to identify involved functional groups of *C. speciosa* tree leave along with their possible interactions with Pb(II) ions. Organic elemental analysis was also performed with an elemental analyzer (Elementary Vario El (III). The XRD spectra of powder of pristine and loaded sorbent were recorded over a range of 15–75˚ using Phillips powder diffractometer model PW3040 with Cu Kα radiation at a scan rate of 1 min. The morphological features and surface characteristics of samples were obtained from SEM using a Philips XL30 Scanning Electron Microscope at an accelerating voltage of 10 kV. The samples were coated with platinum under vacuum prior to analysis.

2.5. Response surface modeling

Response surface methodology (RSM), which includes a group of mathematical and statistical procedures, has recently shown many interesting benefits to be used for process optimization toward developing an appropriate relationship between the responses and effective factors [26]. This study uses the Doehlert design that was used as a RSM, due to its main features such as more efficiency and requiring fewer experiments than central composite design and Box–Behnken design (BBD). Moreover, its ability to take multilevel factors as three, five, and seven is another positive point of its advantage. This characteristic has a particular importance when there are some restrictions in terms of cost or instrumental and experimental constraints. More effective factor is studied at higher level while the less one at lower. The number of the experimental points for a Doehlert matrix for k factors is given by the relation: $k^2 + k + n$, where n is the number of replicate points at the center of the design. Since these points are uniformly distributed on a spherical shell, Doehlert suggested that this design can be called uniform shell design [27]. For statistical calculations, the factor X_i was coded as x_i according to Eq. (3):

$$x_i = \left(\frac{X_i - X_{0i}}{\Delta X_i}\right)\alpha_i \quad (3)$$

where x_i is the coded value of the ith factor, X_i the natural value, X_{0i} the value at the center point, ΔX_i the step change value, and α_i is the maximum value of the coded factor (i.e. 1.0, 0.866 and 0.816 for five, seven, and three levels, respectively) [26].

3. Results and discussion

3.1. Optimization strategy

The optimization process was carried out using a full-factorial design followed with a Doehlert design including three effective factors. In order to explore the best experimental conditions, which lead to maximize the removal percent and the capacity uptake of

Pb(II), an optimization process has been achieved using the desirability function. It was based on four main factors, such as initial solution pH, initial concentration of Pb(II), sorbent mass, and temperature. The results of the factorial design were evaluated using the analysis of variance at 95% confidence level along with Pareto Chart illustration. In Pareto Chart, the bar lengths are proportional to the absolute value of the estimated effects, helping in comparing the relative importance of the factor effects. The experimental data were processed using the MINITAB 15 statistical software.

3.1.1. Factorial design for factor screening

Preliminary evaluation of the significant factors has been conducted by using a full factorial design. The required number of experiments is calculated as $N = 2^k$, where (k) is the number of factors [4,26–28]. According to the prior knowledge, four factors of initial solution pH, initial concentration of Pb(II), sorbent mass, and temperature are considered as main parameters on the removal of Pb(II), and a 2^4 full-factorial design was performed. The results are listed in Table 1, and importance and sequence of effective factors in response is shown in Fig. 1. It is found that pH, concentration of Pb (II)(C_m), and sorbent mass(s) are statistically significant; however, the temperature has not shown a significant effect on the removal efficiency of Pb(II).

Table 1
2^4 full factorial design results for screening step

Run order	pH	s (g)	C_m (mgL^{-1})	t(℃)	R%
1	2	0.05	50	25	80.00
2	5	0.05	50	55	85.00
3	2	0.20	200	25	83.00
4	5	0.05	50	25	84.94
5	2	0.05	200	25	70.00
6	5	0.20	50	25	98.04
7	2	0.20	50	25	99.49
8	2	0.20	200	55	84.14
9	2	0.05	200	55	70.00
10	2	0.20	50	55	100.00
11	5	0.05	200	55	75.00
12	5	0.20	50	55	96.58
13	2	0.05	50	55	80.00
14	5	0.20	200	25	90.06
15	5	0.20	200	55	90.78
16	5	0.05	200	25	75.00

3.1.2. Final optimization using a Doehlert design

According to the output of the full-factorial design, a Doehlert design, including the effective factors, was performed. Seven levels were used for s, since this factor presents greater influence than other two ones (Fig. 1), then for C_m and pH, respectively; five and three levels were appointed (Table 2).

As regression analyses depicted, obtained data via Doehlert design are fitted well with two polynomial equations. The following models, which relate both responses R% and q with significant factors and their interactions, are given in coded value.

$$R\% = 87.78 + 4.66\,s + 0.823\,\mathrm{pH} - 3.50\,C_m + 4.64\,s.C_m - 5.09\,\mathrm{pH}.C_m - 2.73\,s.\mathrm{pH} + 8.36\,\mathrm{pH}.s.C_m - 3.97\,s^2 + 1.68\,s^3 \quad (4)$$

$$q = 8.61 + 4.91\,C_m - 5.35\,s + 0.12\,\mathrm{pH} - 3.82\,s.C_m + 2.33\,s^2.C_m + 0.353\,\mathrm{pH}.C_m + 4.87\,s^2 - 3.60\,s^3 + 0.064\,s^4 \quad (5)$$

$R\%$ and q represent the predicted removal percent and the capacity uptake of Pb(II), respectively. The validity of the models was checked by the Fisher's statistical test for analysis of variance; results are presented in Table 3. It is evident that the both models are highly significant and do not have any lack of fit at a significant level of 5%. The fitness of the model can be illustrated by the coefficient of determination (R^2). The value of R^2 for both responses $R\%$ and q, respectively;

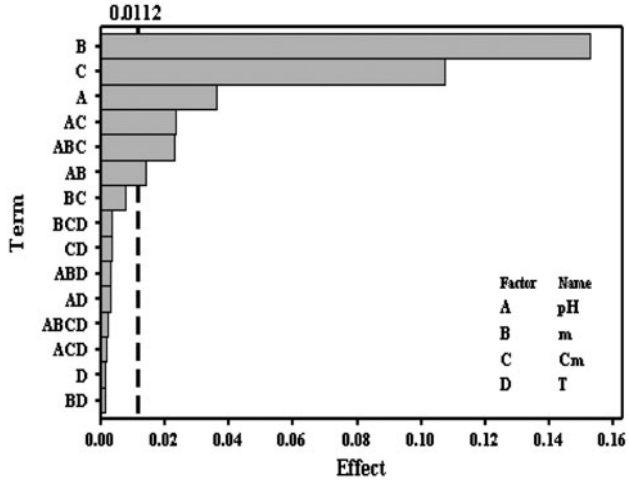

Fig. 1. Pareto chart of the main effects and relation interactions. The vertical dashed line indicates the 95% confidence interval.

Table 2
Doehlert matrix design and obtained results for Pb(II) biosorption using *C. speciosa* tree leaves

Experiment	Coded values			Real values			%R		q	
	x_1	x_2	x_3	S	C_m	pH	Rep. 1	Rep. 2	Rep. 1	Rep. 2
1	0	0	0	0.125	125	3.5	87.57	88.02	8.70	8.60
2	0	1	0	0.125	200	3.5	84.36	84.74	13.50	13.52
3	0.866	0.5	0	0.2	162.5	3.5	90.18	90.13	7.33	7.32
4	0.289	0.5	0.816	0.15	162.5	5	86.38	86.86	9.60	9.63
5	0	−1	0	0.125	50	3.5	91.06	91.74	3.64	3.71
6	−0.866	−0.5	0	0.05	87.5	3.5	83.47	83.61	14.60	14.61
7	−0.289	−0.5	−0.816	0.1	87.5	2	84.19	83.85	7.55	7.63
8	−0.866	0.5	0	0.05	162.5	3.5	75.91	75.86	24.67	24.50
9	−0.289	0.5	−0.816	0.1	162.5	2	85.07	85.54	13.50	13.50
10	0.577	0	−0.816	0.175	125	2	89.96	90.06	6.43	6.42
11	0.866	−0.5	0	0.2	87.5	3.5	89.54	90.00	3.92	4.03
12	0.289	−0.5	0.816	0.15	87.5	5	91.00	90.91	5.31	5.37
13	−0.577	0	0.816	0.075	125	5	85.53	85.12	14.26	14.12

Table 3
Analysis of variance for adsorption of Pb (II) onto *C. speciosa* tree leaves

Source	DF	R%				q			
		SS	Adj. MS	F	P	SS	Adj. SS	F	P
Regression	9	431.946	47.9940	644.534	0.000	802.308	89.145	29512.2	0.000
s	1	260.848	18.6563	250.544	0.000	462.559	24.605	8145.5	0.000
C_m	1	72.161	73.3332	984.827	0.000	232.996	134.048	44377.4	0.000
pH	1	4.194	5.0436	67.732	0.000	0.898	0.112	37.2	0.000
s.pH	1	2.359	9.3030	124.934	0.000			124.934	0.000
pH.C_m	1	15.796	31.0163	416.533	0.000	0.150	0.150	49.6	0.000
pH.s.C_m	1	5.825	5.8252	78.230	0.000			78.230	0.000
s.C_m	1	32.302	32.3019	433.797	0.000	23.118	21.934	7261.4	0.000
s^2	1	37.405	37.4046	502.324	0.000	73.382	2.252	745.4	0.000
s^3	1	1.055	1.0546	14.163	0.002	4.865	4.865	1610.7	0.000
s^4	1					0.025	0.025	8.3	0.011
s^2.C_m	1					4.316	4.316	1428.8	0.000
Error	16	1.191	0.0745	1.442					
Lack-of-fit	3	0.298	0.0992		0.276	0.048	0.003		
Pure error	13	0.894	0.0688			0.005	0.002	0.5	0.662
						0.043	0.003		

Notes: DF = degree of freedom; SS = sum of squares; Adj. MS = adjusted mean square (SS/DF); F: Fischer ratio; P: significance level significance.

is greater than 99% and approximately 100. It should be noted that the R^2 value represents the percentage variation in the response explained by the deliberate variation of the factors in the course of the experiment. Moreover, the value of adjusted R^2 was also high for both responses (> 99%), showing again the high significance of the models [23,28]. The residual analysis also confirms the validity of models (Figure is not shown). Finally, the values of optimal conditions for effective factors were found by running, the Maple optimization toolbox. The maximum value of *R* % is achieved to 99% in pH = 5, *s* = 0.182 g and C_m = 50 mg L^{-1}. The *q* value corresponding to this condition is 2.67 mg g^{-1}. The maximum value of *q* is 29.94 mg g^{-1} at pH = 5, s = 0.05 g and C_m = 200 mg L^{-1}, which corresponds to *R* = 74.85%. As can be seen, the maximization of each response cannot be attainable at the same conditions. The maximum value for R% is in low concentration of Pb(II) and high sorbent amount(s), while the maximum value for q is acquired at reverse order of conditions. So the simultaneous maximization of both responses, R% and *q*, requires to apply a multicriteria decision approach, for instance a desirability function [12,26].

3.1.3. Simultaneous optimization using desirability function

The careful analysis of the response surface plots reveals that the considered factors in most cases have an opposite influence on the considered responses. In order to overcome this conflict and to find a good compromise among the responses, Derringer's desirability function (D) was used [23,28,29]. Each response has to be transformed into a partial desirability function d_i corresponding to defined optimization criteria, and then, an overall desirability function D is calculated by using the geometric mean approach. D function and the partial desirability d_i, were calculated by means of the NEMRODW software. With calculation of total desirability function $(D = \sqrt{d_1 d_2})$, the most removal percent R% and the capacity uptake q of Pb(II) were found to be in optimum conditions as: pH = 4.4, s = 0.07 g and C_m = 104 mg L^{-1}. The R% and q values found based on these conditions are 86% and 14.7 mg g^{-1}, respectively. Contour plots from modeling the overall desirability function can be seen in Fig. 2. These plots clearly show the interaction between effective factors and region of optimum conditions.

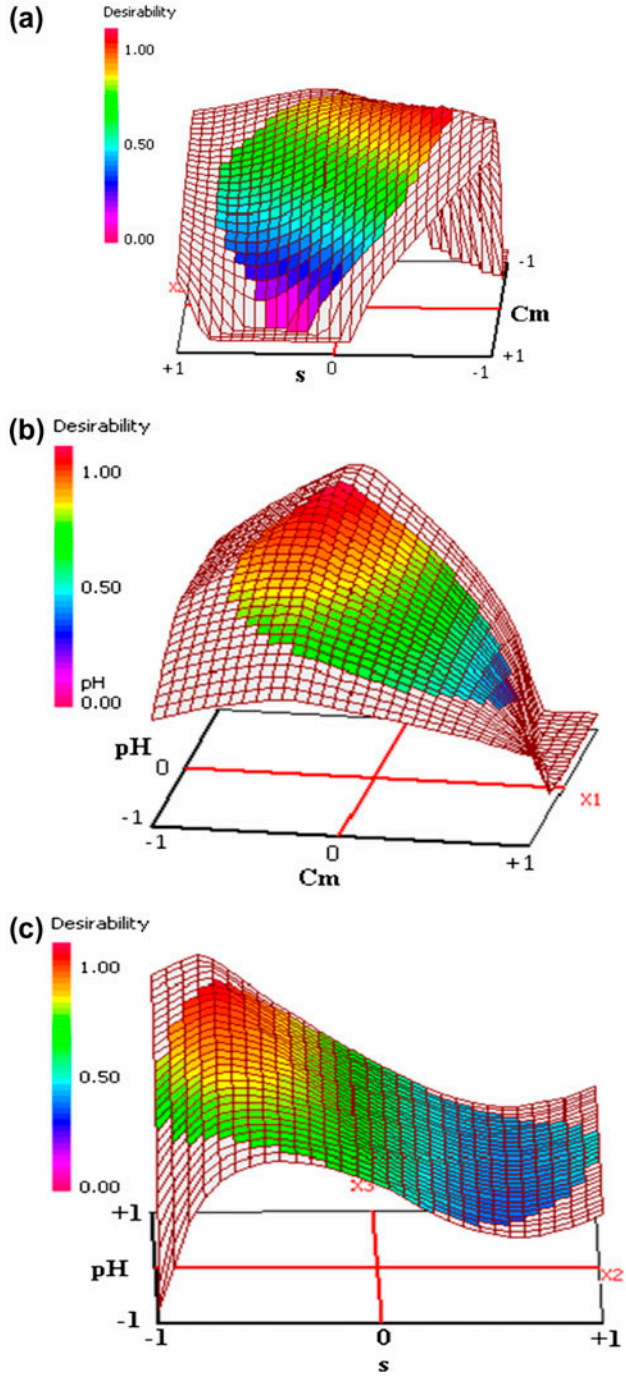

Fig. 2. Three-dimensional plot of desirability function obtained by plotting: (a) sorbent mass (s) vs. Pb(II) concentration(C_m); (b) Pb(II) concentration (C_m) vs. pH and (C_m) pH vs. sorbent mass (s).

3.2. Surface characterization

3.2.1. Potentiometric titration

Potentiometric titration method was used to characterize *C. speciosa* tree leaves with obtaining information about chemical nature and concentration of active sites involved in metal removal. Accordingly, experimental data were elaborated with an original chemical model. So the experimental data of potentiometric titration of *C. speciosa* tree leave was expressed as concentration of surface charge (Q, mmol g^{-1}) vs. pH of bulk solution (Fig. 3). Regarding the charge balance in the system, equation below can be written:

$$[Na^+]_{added} + [H^+] = Q + [OH^-] + [Cl^-]_{added} \quad (6)$$

where the concentration of added Na^+ is equal to V_bC_b/V_T and the concentration of Cl^- equals to V_aC_a/V_T, with inserting these terms in Eq. (6) leads to the following equation:

$$Q\left(\frac{mol}{g}\right) = \frac{(V_b \cdot C_b - V_a \cdot C_a) + \left([H^+] - \frac{Kw}{[H^+]}\right) \cdot V_T}{s} \quad (7)$$

while V_b(L) and V_a(L) are added base and acid volumes, C_b(M) and C_a(M) are the base and acid concentrations (mol L^{-1}), V_T is the total volume (L) of the suspension after each titrant addition, s is the sorbent mass (g) and K_W denotes the ionization constant of water. As seen in Fig. 3, titration curve of *C. speciosa* tree leaves does not show distinct flex points due to

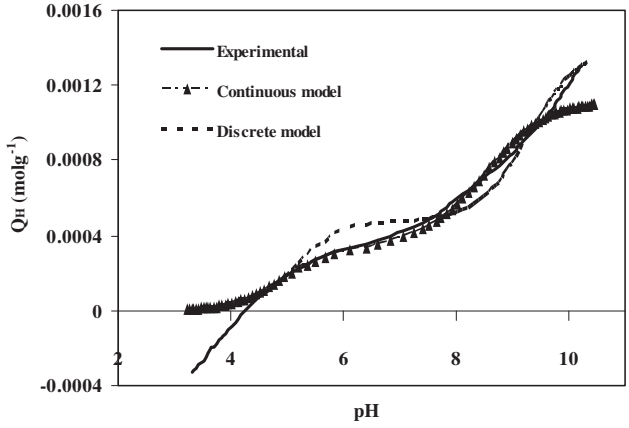

Fig. 3. Comparison among experimental data of potentiometric titration and discrete and continuous model predictions for *C. speciosa* tree leave.

the site dissociation. It can be due to the dissociation of weak acid functional groups. As a primary approximation, it was considered that there are two weak acidic sites (S_1, S_2) on the tree leaves. Total charge is the sum of charges of two different sites, which are assumed to be monoprotic. For *j*th site with dissociation constant K_{aj}, the following equations are applied [30–33]:

$$[H^+] + [B_j^-] \leftrightarrow [BH_j] \quad K_{aj} = \frac{[H^+][B_j^-]}{[BH_j]} \tag{8}$$

$$[B_{Tj}] = [B_j^-] + [BH_j] \tag{9}$$

The charge can be calculated by combining Eqs. (8) and (9) for *j* sites:

$$Q_H = \sum_{j=1}^{2} \frac{Q_{\mathrm{Max},j}}{1 + (K_{H,j}[H^+])} \tag{10}$$

$Q_{max,1}$, $Q_{max,2}$ (mol g^{-1}) are the total concentration of first and second sites of functional groups existing in the biosorbent. To evaluate four constants ($Q_{max,1}$, $Q_{max,2}$, $K_{H,1}$, $K_{H,2}$) a nonlinear regression method was used to solve the Eq. (10) using Microsoft Excel (Solver Toolbox). Two buffering capacities in Fig. 3 denote acid–base reactions occur in the range of pH 3–5 and 8–10, which the literature lists for Carboxylic and Phenolic groups. As could be observed from Fig. 3, the calculated protonation curve from continuous model fits better to the experimental data points than discrete model. It suggests that the biosorbent surface has a heterogeneous distribution of carboxylic and hydroxyl groups. Based on equations established by Pagnanelli [30,31], the continuous model is introduced as follows:

$$Q_H = \frac{Q_{\mathrm{Max},1}}{1 + (\overline{K}_{H,1}[H^+])^{m1}} + \frac{Q_{\mathrm{Max},2}}{1 + (\overline{K}_{H,2}[H^+])^{m2}} \tag{11}$$

where $\overline{K}_{H,1}$ and $\overline{K}_{H,2}$ are the median value of the first and second peak distribution, m_1 ($0 < m_1 < 1$) is the parameter related to the shape of distribution (if m_1 decreases, the distribution will become more disperse). The obtained parameters resulted from fitting are tabulated in Table 4. As can be observed, the negative logarithm of the equilibrium constant (pK_H) for proton binding of the first group was estimated to be 4.9 ± 0.08 which corresponds to carboxyl group (S–COOH) and varies pK_H values in a range from 3.5 to 5. The pK_H value of the second site was estimated to be 9 ± 0.06 that may be attributed to the presence of hydroxyl (phenol) groups (S–OH) in the cell wall of sorbent [32,33]. The number of first and second acidic sites are, respectively, 0.29 ± 0.01 and 0.82 ± 0.02 mmol g^{-1}.

Table 5
Results of elemental analysis of *C. speciosa* tree Leave

Element	%
C	43.09
H	5.50
N	2.79
O	48.62

3.2.2. Biosorbent characterization by FT-IR, XRD, SEM, and elemental analysis

The elemental analysis result of *C. speciosa* tree leave is given in Table 5. It shows that the amount of

Table 4
Values of adjustable parameters for discrete and continuous models of *C. speciosa* tree leave titration curves

	$Q_{max,1}$ (mmol g^{-1})	$Q_{max,2}$ (mmol g^{-1})	pK_1	pK_2	m_1	m_2
Discrete model	0.48	0.93	5.29	9.38	—	—
Continuous model	0.29	0.82	4.90	9.00	1	0.5

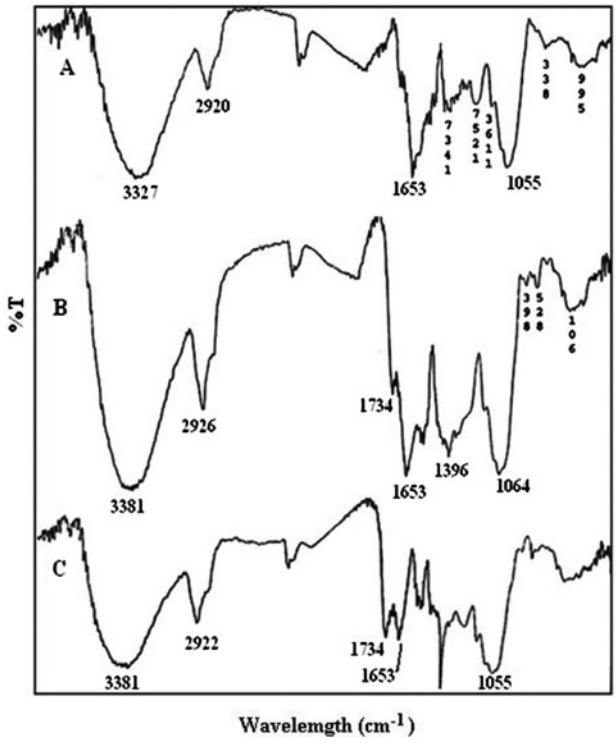

Fig. 4. FT-IR spectra of pristine (A), Pb (II) loaded (B) and protonated *C. speciosa* (C).

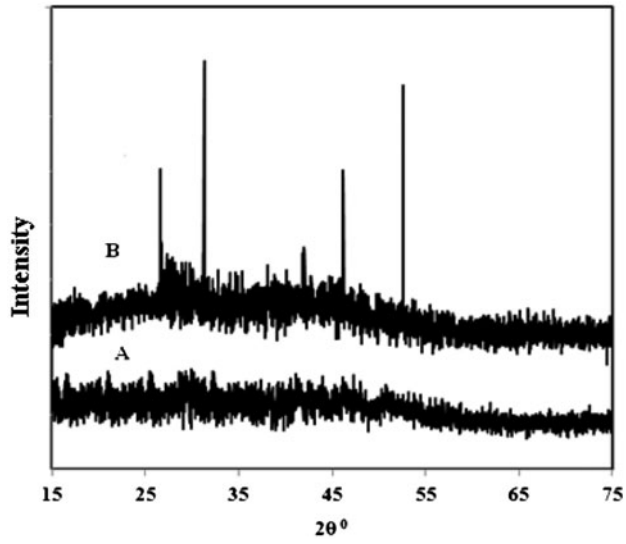

Fig. 5. XRD spectra of pristine (A) and Pb (II) loaded onto *C. speciosa* (B).

oxygen and nitrogen are significant in biosorbent, and they appeared in form of oxy-functional groups such as C–O, C=O, O–H and nitrogen as C–N and N–H in it. FT-IR analysis was conducted with protonated, Pb-loaded, and pristine *C. speciosa* tree leaves in order to identify the groups involved in the adsorption of Pb(II) (Fig. 4). The protonated *C. speciosa* tree leaves can be treated as a reference. The peaks at 3,327, 2,920, 1,653, 1,257, and 1,055 cm^{-1} were observed in the pristine biomass spectrum (Fig. 4(a)). The broad and strong band ranging from 3,000 to 3,700 cm^{-1} should be attributed to the overlap of O-H and N–H stretching vibrations. The peaks at 1,055 and 1,257 cm^{-1} assigned to be C–O and C–N stretching vibrations, thus these infer the presence of hydroxyl and amine groups on the biosorbent surface. Also peak at 1,653 cm^{-1} could be assigned to be a stretching vibrations of ionic carboxylic groups ($–COO^-$) like –COONa. As seen in Fig. 4(b), after contacting the biomass with HCl, the intensity of band at 3,381 cm^{-1} corresponding to the O–H stretching vibrations increased due to the conversion of carboxylate ions to the carboxylic acid. The spectra of protonated and Pb-loaded biomass (Fig. 4(c)) typically display the same absorbance peaks at 3,381, 1,734, and 1,653 cm^{-1}. The peak at 1,734 cm^{-1} corresponds to the stretching vibrations of C=O due to nonionic carboxylic groups (–COOH, $–COOCH_3$). Comparison of the spectra obtained from lead addition with pristine biomass shows an increase in intensity and a clear shift in wave number of the O–H and C–O bands from 3,327 to 3,381 cm^{-1} and 1,055 to 1,064 cm^{-1}, respectively. These shifts may be related to the complexation of hydroxyl band with lead ions. In addition, intensity of peaks at 1,734 and 1,653 cm^{-1} increased due to binding of divalent cations through ionic exchange [34–36].

Additional studies were carried out using XRD analysis to confirm the adsorption of the Pb(II) by *C. speciosa* tree leaves (Fig. 5). X-ray powder diffraction patterns were compared with the reference database for metallic lead. The XRD analysis of active cells shows clear peaks of lead at 2θ = 31.31, 46.23 and 52.61, which confirms the existence of lead ions on the loaded biosorbent [37].

3.2.3. Scanning electron microscopy

Sorbent's surface physical morphology before and after Pb(II) biosorption was evaluated by SEM micrographs. SEM images of unloaded and Pb-loaded adsorbent at 2,500 times of magnification are presented in Fig. 6(a) and (b), respectively. The surface of biosorbent has irregularly been dispersed by granules and cavities, and there are some micropores on the rough surface. When adsorption process took place, the surface of structure of biosorbent slightly changed and became rough. New shiny bulky small particles cover on the corrugated surface of biomass, which

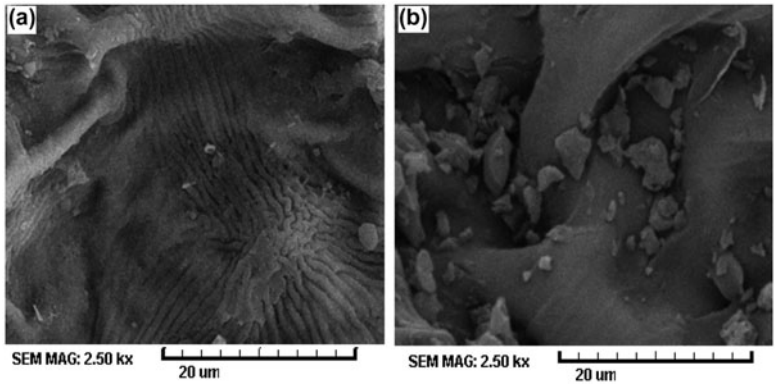

Fig. 6. SEMs of *C. speciosa* tree leave a) before and b) after loading by Pb (II).

may be attributed to the coverage of the surface by a layer of Pb(II).

3.3. Effect of pH on Pb(II) adsorption

It is well known that pH of the medium is among the most important factors which influencing the biosorption process [38]. The solution's pH value affects degree of ionization of functional groups, the surface charge, and the speciation of lead, all of which can affect the adsorption mechanism and the uptake capacity [38,39]. It can be seen from Eqs. (4) and (5) that increasing both $R\%$ and q values occurs when the pH of solution goes up from 2 to 5 (sign of pH is positive). The influence of the solution's pH on metal ion uptake can be explained on the basis of the pH at point of zero charge (pH_{PZC}). The pH_{PZC} of a material in a solution is the pH value at which the net surface charge of this material is equal to zero [39]. Generally, at $pH > pH_{PZC}$, the adsorption of cations is favorable, while the anions are better adsorbed at $pH < pH_{PZC}$. The pH_{PZC} of *C. speciosa* tree leaves is found to be 4.74 in this study (the crossover point in Fig. 3). It means at pH < 4.7, due to protonation of functional groups the surface of *C. speciosa* tree leave has a net positive charge. According to Table 3, the highest investigated pH of solution is 5, which it is so close to the pH_{PZC}. So the portion of electrostatic attractions in the adsorption of Pb (II) from aqueous solution in this pH range is dispensable [20,36,40]. Both IR spectra and the potentiometric titration plot, confirm that *C. speciosa* tree leaves are containing carboxylic and hydroxyl groups. The carboxylic groups are protonated at low pHs and thereby become unavailable for binding metal ions. Hydroxyl groups only become negatively charged at pH > 9, and play a secondary role in metal binding at low pHs [40]. An increase in biosorption capacity by growing the pH can be explained by ion-exchange mechanism. At highly acidic pHs, a high concentration of H^+ ions competes with Pb(II) for exchangeable sites on the surface of adsorbent, resulting in poor uptake of Pb(II) on *C. speciosa* tree leave surface. With increasing pH, more exchangeable sites on the surface of adsorbent can be replaced with Pb (II) due to weaker competitive adsorption of H^+ ions which consequently causes an increase in Pb(II) uptake. Moreover, the chemical speciation of metal ions is determined by pH of solution. The speciation of lead is shown in the following pattern: Pb(II) as dominant species at pHs < 5.5, $Pb(OH)_4^{2-}$ at pHs above 12.2 and $Pb(OH)_2$ at pH from 5.5 to 12.5 [20,39].

3.4. Adsorption isotherms

The analysis of equilibrium data is necessary to compare behavior of different adsorbents under different operational conditions as well as design and optimization of a process. Many equations have been driven to describe the equilibrium relationship between adsorbed metal ions and metal ions in the bulk of solution [41]. In this study, to provide the best description of Pb(II) adsorption, two and three parameters of adsorption models were experienced and isotherm parameters were estimated by nonlinear regression method (Table 5) [41,42]. In order to manifest an agreement between equilibrium models and experimental data, applying an error function is required. For this purpose, normalized standard deviation (Δq), coefficient of determination (R^2), Chi-square (χ^2), the residual or sum of square error (SSE), and the standard error (SE) statistics need to be calculated as follows:

$$\Delta q = \sqrt{\frac{\sum \left[(q_{e,\exp} - q_{e,cal})/q_{e,\exp}\right]^2}{n-1}} \quad (12)$$

$$R^2 = \sum (q_{e,\exp} - \overline{q}_{calc})^2 / \sum \left((q_{e,\exp} - \overline{q}_{calc})^2 + (q_{e,\exp} - q_{calc})^2 \right) \quad (13)$$

$$\chi^2 = \sum \frac{(q_{e,\exp} - q_{e,cal})^2}{q_{e,cal}} \quad (14)$$

$$\mathrm{SSE} = \sum_{i=1}^{m} (q_{e,\exp} - q_{e,cal})^2 \quad (15)$$

$$\mathrm{SE} = \sqrt{\frac{1}{(m-p)} \sum_{i=1}^{m} (q_{e,\exp} - q_{e,cal})^2} \quad (16)$$

High R^2 value and low values of χ^2, Δq, SSE, SE indicate apparently that the model fits the data well.

3.4.1. Two-parameter isotherms

In the present study, two parameter isotherm models, namely Langmuir, Freundlich, Dubinin-Radushkevich(D–R), Temkin, and Halsey were used [41,42]. The Langmuir isotherm is valid for monolayer adsorption on a surface containing finite number of identical sites which assumes the adsorption of each molecule onto the surface has equal adsorption activation energy. In contrast, the Freundlich isotherm supposes a heterogeneous surface with a nonuniform distribution for the heat of adsorption over the surface which a multilayer adsorption can be expressed. The Langmuir and Freundlich isotherms are expressed as Eqs. (17) and (18), respectively [41,43]:

$$q_e = \frac{Q_m b C_e}{1 + b C_e} \quad (17)$$

$$q_e = K_F C_e^{1/n} \quad (18)$$

where q_m is the maximum amount of adsorption (mg g^{-1}), q_e is the adsorption capacity at equilibrium (mg g^{-1}), b is the adsorption equilibrium constant (L mg^{-1}), C_e is the equilibrium concentration of sorbate in the solution (mg L^{-1}), K_F is the constant representing the adsorption capacity, and n is the constant depicting the adsorption intensity.

Unlike the Langmuir and Freundlich equations, the Temkin isotherm takes into account the interactions between adsorbents and metal ions which to be adsorbed. It is based on the assumption that the free energy of sorption is a function of the surface coverage [44]. The isotherm is as follows:

$$q_e = \frac{RT}{b} \ln(a C_e) \quad (19)$$

where a is the equilibrium binding constant corresponding to the maximum binding energy, b is the Temkin isotherm constant, T is the temperature (K), and R is the ideal gas constant.

The Dubinin–Radushkevich (D–R) isotherm is more general than the Langmuir isotherm, because it does not assume a homogeneous surface or constant sorption potential [41]. The D–R equation is given below:

$$q_e = q_{\max} \exp\left(-B[RT \ln(1 + 1/C_{eq})]^2\right) \quad (20)$$

where B is a constant related to the adsorption energy, R (8.314 $Jmol^{-1}$ K^{-1}) is the gas constant, and T (K) is the absolute temperature. The constant B (mol^2 kJ^{-2}) gives the mean free energy E (kJ mol^{-1}) of sorption per molecule of the sorbate, when it is transferred to the surface of the solid from infinity in the solution and can be calculated using the relationship

$$E = 1/(2\beta)^{1/2} \quad (21)$$

This parameter imparts information about chemical or physical adsorption. If the magnitude of E lies between 8 and 16 kJ mol^{-1}, the biosorption process follows chemical ion-exchange, while for the values of $E < 8$ $kJmol^{-1}$ the biosorption process turns to a physical nature [41–43]. The mean free energy of Pb(II) biosorption was found to be 12.91 kJ mol^{-1} which indicates that one of the mechanisms for the biosorption of Pb(II) onto biomass may be a chemical ion exchange. This is confirmed by n obtained from Freundlich isotherm (0.34) which implies that chemisorptions has taken place [44].

The Halsey adsorption isotherm can be given as follows:

$$q_e = \exp\left(\frac{\ln K_H - \ln C_e}{n}\right) \quad (22)$$

where K_H and n are the Halsey isotherm constant and exponent, respectively. This equation is suitable to describe a multilayer adsorption which fitting the experimental data to this equation attests to the heterogonous nature of the adsorbent [41,42,44]. Fig. 7(a) shows a comparative analysis of the experimental data with all the two parameter models.

Between the two-parameter isotherms, the Langmuir model exhibits the best fitting to the experimental data which may be deduced from its highest R^2 and least values of other statistic parameters (χ^2, SSE, SE) (Table 6). Therefore, the adsorption of Pb(II) on *C. speciosa* tree leaves can be homogeneous and monolayer.

3.4.2. Three-parameter isotherm models

In this section, Redlich–Peterson, Sips, and Toth isotherms were used to model the experimental data. The three-parameter models express the adsorption capacity, q_m, as an inherent function of the equilibrium concentration and are empirical in nature [44,45].

The Redlich–Peterson (R–P) isotherm is an empirical isotherm incorporating three parameters. It combines elements from both the Langmuir and Freundlich equations, and the mechanism of adsorption is a hybrid and does not follow ideal monolayer adsorption. This model gives a more realistic representation of an adsorption system operating over a wide range of concentrations. R–P model can be represented as follows:

$$q = \frac{KC_{eq}}{1 + aC_{eq}^{\beta}} \tag{23}$$

where K, a and β are the R–P parameters. β lies between 0 and 1. For $\beta = 1$, the R–P equation convert to Langmuir form. When K and a are much greater than unit value, the equation can be transformed to Freundlich form [44,45].

Toth isotherm model is another empirical equation developed to improve Langmuir isotherm fittings (experimental data), and useful in describing heterogeneous adsorption systems, which satisfies both low and high-end boundary of the concentration. The Toth model equation given as [41,42,44]:

$$q_e = \frac{q_{\max}\, b_T C_{eq}}{\left[1 + \left(bC_{eq}\right)^n\right]^{\frac{1}{n}}} \tag{24}$$

where b is the Toth model constant, and n is the Toth model exponent. Obviously, if $n = 1$ Eq. (24) reduces to Langmuir type equations but the Toth but could not reflect the feature of the Freundlich-type biosorption [41].

The Sips model equation given as

$$q = q_{\max} \frac{(k\, C_{eq})^{\gamma}}{1 + (k\, C_{eq})^{\gamma}} \tag{25}$$

Sips equation has similar form to Langmuir equation. A distinctive feature between these isotherms is the presence of additional parameter, γ in Eq. (25). If this parameter takes a unity, Sips equation resembles Langmuir equation. The parameter γ is regarded as the characterizing parameter of the system's heterogeneity. Moreover, the heterogeneity could stem either from the biosorbent or the heavy metal, or a combination of both [41,42,44]. Fig. 7(b) shows a comparative analysis of the experimental data with the three parameters model. As shown in Table 5, all three-parameter equations provide a better fit of the isotherm data than two-parameter ones. Based on the results of the study, best isotherm models fitted for Pb (II) biosorption was determined as following order: Sips > Toth > R–P. The highest coefficient of determination for Sips model suggests that the surface of adsorbent is heterogenic and the mechanism of adsorption is a combination of Langmuir and Freundlich isotherms and does not follow ideal monolayer adsorption.

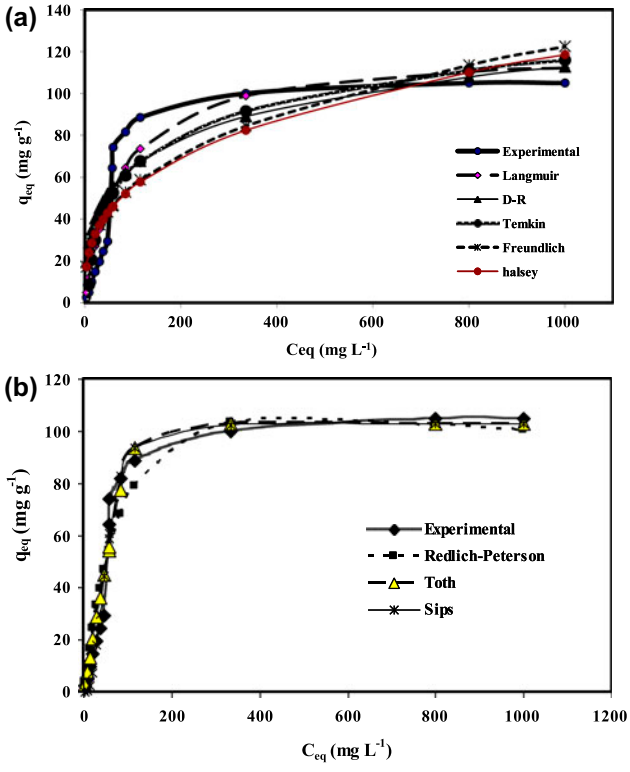

Fig. 7. Non-linear fits of (a) two-parameter isotherm models and (b) three-parameter isotherm models for Pb (II) onto *C. speciosa* tree leaves (t = 25°C; pH = 5; s = 0.189 g).

Table 6
Constant parameters and different criteria calculated for nonlinear fitting of various adsorption isotherms

Isotherm models	Constants	Parameter values	R^2	Δq	χ^2	SSE	S.E.
Langmuir	q_{max} (mg g^{-1})	120.19	0.90	0.69	54.7	2293.47	13.82
	b (L mg^{-1})	0.014					
Freundlich	K_f (mg g^{-1})	11.70	0.79	2.09	129.23	5438.80	21.29
	n	0.34					
Dubinin–Radushkevich	q_{max} (mg g^{-1})	190.62	0.80	2.5	483.35	5321.16	21.06
	B(mol^2($kJ)^{-2}$)	3×10^{-9}					
Temkin	a (L mg^{-1})	0.18	0.86	1.9	47.02	3339.82	16.68
	b (kJ mol^{-1})	111					
Halsey	K	6×10^{-4}	0.79	2.1	132	5641.02	21.68
	n	−3					
Redlich-Peterson	a (1/mg)	0.003	0.92	0.54	13,251	1733.33	12.55
	β	0.95					
	K(L g^{-1})	1.3					
	q_{max} (mg g^{-1})	102.94	0.97	0.48		666.33	7.78
Sips	k(Lmg^{-1})	0.019			278.77		
	γ	2.87					
Toth	q_{max} (mg g^{-1})	102.75	0.95	0.34	24.67	1032.50	9.69
	b (L mg^{-1})	9.3×10^{-3}					
	n	5.56					

3.5. Kinetic modeling

Kinetic studies of adsorption for Pb(II) onto *C. speciosa* tree leaves were carried out at the initial concentrations of 150.0 mg L^{-1} for a contact times of 5–180 min. As can be seen in Fig. 8, the adsorption of Pb(II) is rapid and an interaction period of 5 min supplies about 72% adsorption, whereas the equilibrium condition was reached at approximately 70 min. In this study, the biosorption kinetics were investigated by using kinetic models such as Lagergren's pseudo-first-order, the pseudo-second-order, Boyd and the intraparticle diffusion models [42,46–48]. The pseudo-second-order kinetic model is expressed as below:

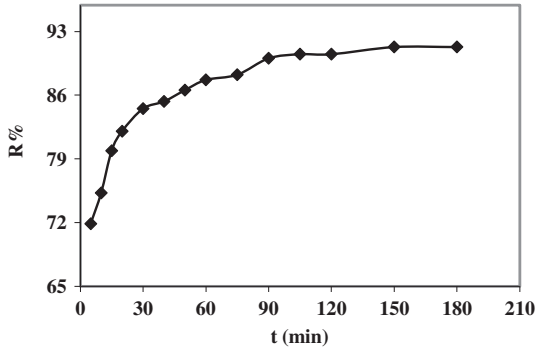

Fig. 8. The effect of contact time on Pb (II) removal percent (t = 25°C; s = 0.189 g; pH = 5; initial conc. of Pb(II) = 150 mg L^{-1}) and pseudo second order kinetics plot for the sorption of Pb(II) onto *C. speciosa* tree leave.

$$\frac{t}{q_t} = \frac{1}{k_2 q_2^2} + \frac{1}{q_2} t \tag{26}$$

where q_2 is the maximum capacity uptake (mg g^{-1}) for the pseudo-second-order biosorption, q_t is the amount of Pb(II) adsorbed at time t (mg g^{-1}), and k_2 is the pseudo-second-order kinetic rate constant (g mg^{-1} min^{-1}). Values of k_2 and q_2 are calculated from the plot of t/q against t and are 0.027 (g mg^{-1} min^{-1}) and 13.89 (mg g^{-1}), respectively. The coefficient of determination R^2 for the pseudo-first-order model and the pseudo-second-order model are 0.86 and > 0.99, respectively. This implies that the adsorption of Pb(II) onto *C. speciosa* tree leave does not properly meet the first-order kinetic model condition. However, the pseudo-second-order kinetic model is more appropriate to predict kinetic behavior of Pb(II) adsorption.

Most adsorption process takes place through multi-step mechanism comprising; (i) external film diffusion, (ii) intraparticle diffusion and (iii) interaction between adsorbate and active sites. The two equations given above are not able to identify the diffusion mechanism; the intraparticle diffusion model that refers to the theory proposed by Weber and Morris is thus tested. This theory is given as following equation [42,49,51]:

$$q_t = k_i t^{1/2} \tag{27}$$

where q_t is the uptake at any time (mg g^{-1}), and k_i is the intraparticle diffusion constant (mg $g^{-1}.min^{0.5}$). Based on this theory, a plot of q_t vs. $t^{1/2}$ should be linear if intraparticle diffusion is involved in the adsorption process, and if this line passes through the origin, then intraparticle diffusion is the rate-controlling step [42,49–51].

Fig. 9(a) presents multilinearity plot which illustrates aforementioned three steps took place during the adsorption process of Pb(II). The initial sharper section in figure may be considered as external surface adsorption, in which the sorbate (Pb(II)) diffuses through the solution to the external surface of the adsorbent. The second section describes the gradual adsorption stage, where the intraparticle diffusion rate is rate-controlling step. The third section is attributed to the final equilibrium stage, where intraparticle diffusion starts to slow down due to the extremely low adsorbate concentrations in the solution [44–46].

In order to determine actual determining step rate of Pb(II) sorption on *C. speciosa* tree leave, the obtained data were also analyzed using the Boyd model [42,49].

$$F = 1 - \frac{6}{\pi^2}\exp(-Bt) \tag{28}$$

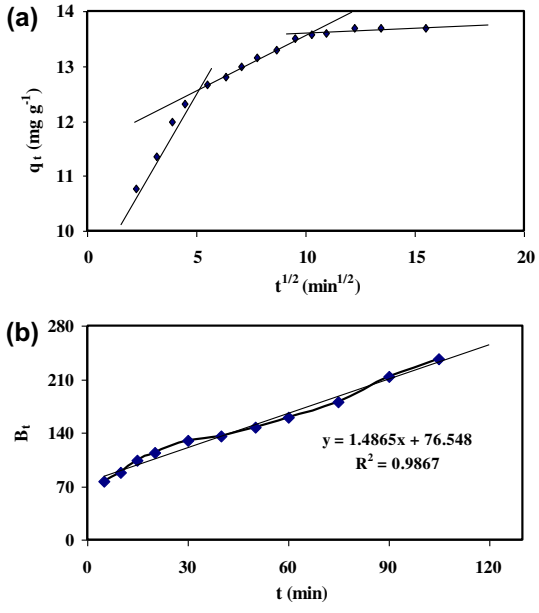

Fig. 9. (a) Intra-particle diffusion and (b) Boyd film diffusion kinetics for adsorption of Pb(II) onto *C. speciosa* tree leave.

where F is the fractional attainment of equilibrium, at different times, t, and B_t is a function of F.

$$F = q_t/q_e \tag{29}$$

where q_t and q_e are the Pb(II) uptake (mg g^{-1}) at time t and at equilibrium, respectively. Eq. (28) can be rearranged to

$$B_t = -0.4977 - \ln(1 - F) \tag{30}$$

The calculated B_t values are plotted against time. The linearity of this plot provides available information to distinguish intra-particle diffusion and external mass transfer rates of adsorption [42]. If a plot of B_t vs. t becomes a straight line passing through the origin, then adsorption fits the external external mass transfer [47–51]. The plot shown in Fig. 9(b) is linear only in the initial period of adsorption process and do not pass through the origin. This Figure indicates that external mass transfer is the rate-limiting process at the beginning of the adsorption process.

3.6. Thermodynamic parameters

Thermodynamic behavior of the adsorption of of Pb(II) sorption on *C. speciosa* tree leaves was evaluated by finding thermodynamic parameters including the changes in free energy and entropy. These factors must be considered in order to determine what processes will occur spontaneously [41–43]. The Gibbs free energy change ΔG° is the fundamental criterion of spontaneity. The free energy change (ΔG°), enthalpy change (ΔH°), and entropy change (ΔS°) for adsorption process by biosorbent were calculated using following equations:

$$\Delta G^\circ = -RT \ln K_c \tag{31}$$

$$\ln K_c = \Delta S^\circ/R - \Delta H^\circ/RT \tag{32}$$

where K_c is the equilibrium constant that can be calculated from Langmuir isotherms at different temperatures. ΔH° and ΔS° were obtained from the slope and intercept of van't Hoff plot of ln K_c against $1/T$. The values of ΔH° and ΔS° were found as 6.97 kJ mol^{-1} and 39.91 $J(Kmol)^{-1}$, respectively. The positive value of ΔH° illuminates the endothermic nature of adsorption and the positive value of ΔS° suggests the increase in randomness at the solid/solution interface during the adsorption of Pb(II) onto *C. speciosa* tree

leaves [5,49]. The negative values of ΔG° at various temperatures approve that the adsorption processes are spontaneous. The values obtained for ΔG° in biosorption of Pb(II) onto *C. speciosa* tree leaves are −4.94 kJ mol^{-1} at 25°C [17,41,42,48,50].

3.7. Biosorption mechanism and competitive effect of alkaline and alkaline earth metal ions

To explain the behavior of Pb(II) adsorption during the pH variation, it is necessary to examine various mechanisms such as electrostatic attraction/repulsion, chemical interaction and ion-exchange, which are responsible for adsorption on adsorbent surfaces. In this study, FT-IR spectra and potentiometric investigation show *C. speciosa* tree leave contain some active adsorption sites. It is proposed that, when heavy metal ions appear in the solution, protons and/or alkali and alkaline earth metals presenting in the biomass will be exchanged from these binding sites with heavy metal ions and which the process of ion-exchange will take place. In order to precisely determine the contribution of ion-exchange mechanism of Pb (II) adsorption process, the releasing amount of alkali and alkaline earth metal ions (K^+, Na^+, Ca^{2+}, and Mg^{2+}) originally present in the *C. speciosa* tree leaves, and proton H^+ during adsorption were determined. By subtracting the released amount of these cations before and after loading of Pb(II), the contribution of these cations in ion-exchange mechanism can be achieved [35]. The amount of released proton H^+ during the adsorption of Pb(II) was calculated from the amount of NaOH, which added to maintain pH at 5 until reaching to the equilibrium. It was observed that on contacting 200 mg L^{-1} of Pb(II) with *C. speciosa* tree leaves, 0.163 meq g^{-1} of Pb(II) was adsorbed, while a sum of 0.128 meq g^{-1} of Ca^{2+}, Mg^{2+}, K^+, Na^+ and H^+ is replaced. In other words, only 78% removal of Pb(II) by *C. speciosa* tree leave is due to ion-exchange and the remaining 22% of Pb(II) may be attributed to physical adsorption of Pb(II) onto the surface of *C. speciosa* tree leave [32,35,52]. The D–R isotherm model also confirms that the main mechanism involved in the sorption of Pb(II) by *C. speciosa* tree leave is ion-exchange.

4. Conclusion

The applicability of experimental design through using RSM and desirability function for modeling and multiresponse optimization of Pb(II) removal process by *C. speciosa* tree leaves was evaluated. The Doehlert design was shown to be a suitable response surface to determine the effects of different adsorption factors (pH, initial concentration of Pb(II) and sorbent mass) and their interactions for removal of Pb(II) by *C. speciosa* tree leave. The simultaneous optimization of the multiresponse adsorption process by desirability function indicated that 86% removal of Pb(II) can be attained at the optimal conditions as: pH = 4.40, s = 0.07 g and C_m = 104 mg L^{-1}. The graphical response surfaces analysis was employed for identification and discussion of main and interaction effects of factors on responses. The adsorption isotherm was well fitted by the Sips model indicating heterogeneous surface structure of biosorbent. Kinetic studies also shows better obeying the adsorption of Pb(II) from pseudo-second-order model and intraparticle diffusion is not solely the rate-determining step. FT-IR, XRD spectras and potentiometric investigation justified the involvement of functional groups of biosorbent among the removal process. According to these all considerations, it could be concluded that about 78% of biosorption mechanism of Pb(II) by *C. speciosa* tree leave is handled by chemisorption (ion exchange).

Acknowledgment

The authors would like to acknowledge the Research and Technology Center of Arak University for financial support.

References

[1] E.I. Unuabonah, K.O. Adebowale, B.I. Olu-Owolabi, Kinetic and thermodynamic studies of the adsorption of lead (II) ions onto phosphate-mdified kaolinite clay, J. Hazard. Mater. 144 (2007) 386–395.
[2] M.A. Schneegurt, J.C. Jain, J.A. Menicucci, S.A. Brown, K.M. Kemner, D.F. Garofalo, M.R. Qualick, C.R. Neal, C.F. Kulpa, Biomass byproducts for the remediation of wastewaters contaminated with toxic metals, Environ. Sci. Technol. 35 (2001) 3786–3791.
[3] M. Ronteltap, M. Maurer, W. Gujer, The behavior of pharmaceuticals and heavy metals during struvite precipitation in urine, Water Res. 41 (2007) 1859–1868.
[4] C.H. Lai, C.Y. Chen, B.L. Wei, C.W. Lee, Adsorption characteristics of cadmium and lead on the goethite-coated sand surface, J. Environ. Sci. Health A 36 (2001) 747–763.
[5] A. Naeem, J.B. Fein, J.R. Woertz, Experimental measurement of protons, Cd, Pb, Sr, and Zn adsorption onto the fungal species *Saccharomyces cerevisiae*, Environ. Sci. Technol. 40 (2006) 5724–5729.
[6] V.K. Gupta, A. Rastogi, Biosorption of lead from aqueous solutions by green algae Spirogyra species: Kinetics and equilibrium studies, J. Hazard. Mater. 152 (2008) 407–414.

[7] V.K. Gupta, I. Ali, T.A. Saleh, A. Nayak, S. Agrawal, Chemical treatment technologies for waste-water recycling-an overview, RSC Advances 2 (2012) 6380–6388.
[8] M. Nourbakhsh, Y. Sag, D. Ozer, Z. Aksu, T. Katsal, A. Calgar, A comparative study of various biosorbents for removal of chromium (VI) ions from industrial wastewater, Process Biochem. 29 (1994) 1–5.
[9] B. Volesky, Detoxification of metal-bearing effluents: biosorption for the next century, Hydrometallurgy 59 (2001) 203–216.
[10] V.K. Gupta, R. Jain, S. Varshney, Removal of Reactofix golden yellow 3 RFN from aqueous solution using wheat husk—An agricultural waste, J. Hazard. Mater. 142 (1–2) (2007) 443–448.
[11] J. Zolgharnein, Zh Adhami, A. Shahmoradi, S.N. Mousavi, Optimization of removal of methylene blue by *Platanus* tree leaves using response surface methodology, Anal. Sci. 26 (2010) 111–116.
[12] J. Zolgharnein, A. Shahmoradi, Adsorption of Cr(VI) onto *Elaeagnus* tree leaves: Statistical optimization, equilibrium modeling and kinetic studies, J. Chem. Eng. Data 55 (2010) 3428–3437.
[13] M. Riaz, R. Nadeem, M.A. Hanif, T.M. Ansari, K. Rehman, Pb(II) biosorption from hazardous aqueous streams using *Gossypium hirsutum* (Cotton) waste biomass, J. Hazard. Mater. 161 (2009) 88–94.
[14] A. San, M. Tuzen, Biosorption of Pb(II) and Cd(II) from aqueous solution using green alga (Ulva lactuca) biomass, J. Hazard. Mater. 152 (2008) 302–308.
[15] Y. Zhang, C. Banks, A comparison of the properties of polyurethane immoboilized *Sphagnum* moss, seaweed, sunflower waste and maize for the biosorption of Cu, Pb, Zn and Ni in continuous flow packed columns, Water Res. 40 (2006) 788-798.
[16] A. San, M. Tuzen, Kinetic and equilibrium studies of biosorption of Pb(II) and Cd(II) from aqueous solution by macrofungus (*Amanita rubescens*) biomass, J. Hazard. Mater. 164 (2009) 1004–1011.
[17] A.E. Ofomaja, Intraparticle diffusion process for lead (II) biosorption onto mansonia wood sawdust, Bioresour. Technol. 101 (2010) 5868–5876.
[18] Y. Ho, A.E. Ofomaja, Pseudo-second order model for lead ion sorption from aqueous solutions onto palm kernel fiber, J. Hazard. Mater. B129 (2006) 137–142.
[19] S. Qaiser, A.R. Saleemi, M. Umar, Biosorption of lead from aqueous solution by Ficus religiosa leaves: Batch and column study, J. Hazard. Mater. 166 (2009) 998–1005.
[20] H. Chen, J. Zhao, G. Dai, J. Wu, H. Yan, Adsorption characteristics of Pb(II) from aqueous solution onto a natural biosorbent, fallen *Cinnamomum camphora* leaves, Desalination 262 (2010) 174–182.
[21] B. Volesky, Z.R. Holan, Biosorption of heavy metals, Biotech. Prog. 11 (1995) 235–250.
[22] F. Pagnanelli, S. Mainelli, S.D. Angelis, L. Toro, Biosorption of protons and heavy metals onto olive pomace: Modeling of competition effects, Water Res. 39 (2005) 1639–1651.
[23] D.L. Massart, B.G.M. Vandeginste, L.M.C. Buydens, S. De Jong, P.J. Lewi, J. Smeyers-Verbeke, Handbook of Chemometrics and Qualimetrics, Part A. Elsevier, Amsterdam, 1997.
[24] C. Moreno-Castilla, M.V. López-Ramón, F. Carrasco-Marín, Changes in surface chemistry of activated carbons by wet oxidation, Carbon 38 (2000) 1995–2001.
[25] R. Leyva-Ramos, L.A. Bernal-Jacome, I. Acosta-Rodriguez, Adsorption of cadmium (II) from aqueous solution on natural and oxidized corncob, Sep. Purif. Technol. 45 (2005) 41–49.
[26] M.A. Bezerra, R.E.E. Santelli, P. Oliveira, L.S. Villar, L.A. Esclaleira, Response surface methodology (RSM) as a tool for optimization in analytical chemistry-review, Talanta 76 (2008) 965–977.
[27] D.H. Doehlert, Uniform shell design, Appl. Stat. 19 (1970) 231–239.
[28] S.L.C. Ferreira, R.E. Bruns, E.G.P. da Silva, W.N.L. dos Santos, C.M. Quintella, J.M. David, J.B. de Andrade, M.C. Breitkreitz, I.C.S.F. Jardim, B.B. Neto, Statistical designs and response surface techniques for the optimization of chromatographic systems-review, J. Chromatogr. A 1158 (2007) 2–14.
[29] G. Derringer, R. Suich, Simultaneous optimization of several response factors, J. Qual. Technol. 12 (1980) 214–219.
[30] F. Pagnanelli, S. Mainelli, L. Toro, New biosorbent materials for heavy metal removal: Product development guided by active site characterization, Water Res. 42 (2008) 2953–2962.
[31] F. Pagnanelli, S. Mainelli, L. Bornoroni, D. Dionisi, L. Toro, Mechanisms of heavy-metal removal by activated sludge, Chemosphere 75 (2009) 1028–1034.
[32] K. Chojnacka, A. Chojnacki, H. Go'recka, Biosorption of Cr^{3+}, Cd^{2+} and Cu^{2+} ions by blue–green algae *Spirulina sp*.: Kinetics, equilibrium and the mechanism of the process, Chemosphere 59 (2005) 75–84.
[33] M.A. Martin-Lara, F. Herninz, M. Calero, G. Blzquez, G. Tenorio, Surface chemistry evaluation of some solid wastes from olive-oil industry used for lead removal from aqueous solutions, Biochem. Eng. J. 44 (2009) 151–159.
[34] J.P. Chen, L. Yang, Study of a heavy metal biosorption onto raw and chemically modified *Sargassum* sp, via spectroscopic and modeling analysis, Langmuir 22 (2006) 8906–8914.
[35] M. Iqbal, A. Saeed, S. Iqbal Zafar, FTIR spectrophotometry, kinetics and adsorption isotherms modeling, ion-exchange, and EDX analysis for understanding the mechanism of Cd^{2+} and Pb^{2+} removal by mango peel waste, J. Hazard. Mater. 164 (2009) 161–171.
[36] E. Fourest, B. Volesky, Contribution of sulfonate groups and alginate to heavy metal biosorption by the dry biomass of *Sargassum fluitans*, Environ. Sci. Technol. 30 (1996) 277–282.
[37] T. Takahashi, H.K. Mao, W.A. Bassett, Study of lead up to 180 kb, Carnegie Inst. Washington Yearb. 68 (1969) 251–253.
[38] A. Witek-Krowiak, R.G. Szafran, S. Modelski, Biosorption of heavy metals from aqueous solutions onto peanut shell as a low-cost biosorbent, Desalination 265 (2011) 126–134.
[39] U. Farooq, J.A. Kozinski, M.A. Khan, M.A. Athar, Biosorption of heavy metal ions using wheat based biosorbents—A review of the recent literature, Bioresour. Technol. 101 (2010) 5043–5053.
[40] V.J.P. Vilar, C.M.S. Botelho, J.P.S. Pinheiro, R.F. Domingos, R.A.R. Boaventura, Copper removal by algal biomass: Biosorbents characterization and equilibrium modeling, J. Hazard. Mater. 163 (2009) 1113–1122.

[41] Y. Liu, Y.-J. Liu, Biosorption isotherms, kinetics and thermodynamics—Review, Sep. Purif. Technol. 61 (2008) 229–242.
[42] J. Febrianto, A.N. Kosasih, J. Sunarso, Y.-H. Ju, N. Indraswati, S. Ismadji, Equilibrium and kinetic studies in adsorption of heavy metals using biosorbent: A summary of recent studies—Review, J. Hazard. Mater. 162 (2009) 616–645.
[43] J. Zolgharnein, N. Asanjarani, S.N. Mousavi, Optimization and characterization of Tl(I) adsorption onto modified *Ulmus carpinifolia* tree leaves, Clean-Soil, Air, Water 39 (3) (2011) 250–258.
[44] K.Y. Foo, B.H. Hameed, Insights into the modeling of adsorption isotherm systems, Chem. Eng. J. 156 (2010) 2–10.
[45] M. Brdar, M. Šćiban, A. Takači, T. Došenović, Comparison of two and three parameters adsorption isotherm for Cr(VI) onto Kraft lignin, Chem. Eng. J. 183 (2012) 108–111.
[46] Hu Tang, Weijie Zhou, Lina Zhang, Adsorption isotherms and kinetics studies of malachite green on chitin hydrogels, J. Hazard. Mater. 209–210 (2012) 218–225.
[47] A. Özer, G. Gürbüz, A. Calimli, B.K. Körbahtia, Biosorption of copper (II) ions on *Enteromorpha prolifera*: Application of response surface methodology (RSM), Chemical Engineering Journal 146 (2009) 377–387.
[48] M. Alkan, O. Demirbas, S. Celikcapa, M. Dogan, Sorption of acid red 57 from aqueous solution onto sepiolite, J. Hazard. Mater. 116 (2004) 135–145.
[49] V.K.Gupta, A.Mital, L.Kurup, J.mittal, Adsorption of hazardous dye, erythrosine, over hen feathers, J. Coll. Inter. Sci. 304 (2006) 52–57.
[50] V.K. Gupta, I. Ali, V.K. Saini, Defluoridation of wastewaters using waste carbon slurry, Water Res. 41 (2007) 3307–3316.
[51] M-C.Shih, Kinetic of the batch adsorption of methylene blue from aqueous solutions onto rice husk: effect of acid-modified process and dye concentration, Desalin. Water Treat. 37(2012) 331–336.
[52] M.A.K.M. Hanafiah, H. Zakaria, W.S. Wan Ngah, Preparation, characterization, and adsorption behavior of Cu(II) ions onto alkali-treated weed (Imperata cylindrica) leaf powder, Water Air Soil pollut. 201 (2009) 43–53.